EXPERIMENTAL DEVELOPMENT AND NUMERICAL SIMUTATION OF AN ELECTRO-HYDRAULIC SERVO-ACTUATOR

DINCA L. & CORCAU J. I.

Abstract: *In this paper is developed an electro-hydraulic servo-actuator using the identified parameters of a servo-valve. One follows to obtain a null stationary error and a time response as short as possible. The mathematical model of the servo-actuator is deduced taking account the functional model of the open-centre servo-valve. This model is used for the numerical simulation of the system functioning. The model uses the mass flow ratios in order to obtain a more stable and realistic numerical simulation. It is experimentally studied the behaviour of the servo-actuator with different controllers in the control loop. It is tested one proportional controller and two types of fuzzy controllers. The controllers are implemented in MATLAB/SIMULINK and DATA ACQUISITION TOOLBOX is used for the communication with the data acquisition card. The controllers are tested both experimentally and by numerical simulation. One may say the concordance between the numerical results and the experimental data is quite good.*

Key words: *servo-valve; experimental development; numerical simulation; electro-hydrauic servo-actuator, experimental results*

Authors´ data: Associate Professor PhD **Dinca**, L[iviu]; Senior Lecturer PhD. **Corcau,** J[enica] Ileana, University of Craiova, Decebal, 107, Romania, ldinca@elth.ucv.ro, jcorcau@elth.ucv.ro

This Publication has to be referred as: Dinca L[iviu] & Corcau,J[enica] [I]leana (2013) Experimental Development and Numerical Simulation of an Electro-Hydraulic Servo-Actuator , Chapter 50 in DAAAM International Scientific Book 2013, pp. 831-848, B. Katalinic & Z. Tekic (Eds.), Published by DAAAM International, ISBN 978-3-901509-94-0, ISSN 1726-9687, Vienna, Austria
DOI: 10.2507/daaam.scibook.2013.50

1. Introduction

Hydraulic servo-actuators have a wide application in different industrial branches. Between these applications are the steering systems for the road vehicles direction, the ships rudders and aircraft command surfaces. The first applications at the road vehicles direction mechanism appeared in the ’20 of the last century and had a continuous development. On the aircraft the servo-actuators were used beginning the end of the last word war as mechanic-hydraulic servo-actuators, then with the continuous improvement of the control techniques, the electro-hydraulic servo-actuators were introduced.

In present, the electro-hydraulic servo-actuators development aims on the one hand the electric and hydraulic systems, and on the other hand the automatic control techniques to improve the servo-actuators performances. The current development stage of the hydraulic and electric systems for the servo-actuators may be viewed in (Rydberg, 2008), (Panagiotis, 2002), (Johnsen & Thielecke , 2011), (Dinca & Corcau, 2007), (Ciupitu et. al. 2011), (Prodan et. al. 2011). In (Dinca & Corcau, 2007) is studied an electro-hydrostatic servo-actuator for aircraft. This type of servo-actuator is the most recent used on the aircraft. It is still in development process and only the last generation aircrafts are provided with this kind of servo-actuators.

The modern control techniques used for the servo-actuators behaviour improvement are generally based on fuzzy logic (Precup & Preitl 2005), (Ursu et. al. 2011), neural networks (Ursu et. al., 2011), (Daachi et. al., 2001), adaptive control and others types of controllers (Ursu et. al., 2007), (Yu et. al., 2003), (Ursu & Ursu, 2005), (Vasiliu et. al., 2009), (Niksefat & Sepehri, 2000), (Jong-Hwei & Yung, 2010), (Richard, 2005), (Panagiotis & Papadopoulos, 2003).

One important problem of the hydraulic servo-actuators in general and especially of the mechanic-hydraulic servo-actuators is the stability of the static point. It is well known that in the absence of appropriate constructive measures, in the mechanic-hydraulic servo-actuators may appear high frequency (about 30 – 40 Hz) and low amplitude (about tenths of millimeter) auto-oscillations which apply to fatigue the command chains of the aircraft. One study concerning the stability of the static point is presented in (Ursu et. al., 2008).

The study of the ensemble electro-hydraulic servo-actuator plus the embedded controller is another important direction in the development of a hydraulic servo-actuator. For this purpose are wide used the numerical simulations (Dinca, 2005), (Hietala et. al., 2009), (Mizioka, 2009), (Nakata & Xi, 2011). Another testing method of the aircraft equipment in general and hydraulic servo-actuators particularly is the hardware in the loop technique (Hanzálek et. al., 2009). Less presented problem in the literature, but also very important is the energetic efficiency evaluation (Mare, 2009).

This paper presents the mathematical modelling, the development and the experimental validation of an electro-hydraulic servo-actuator, starting from the identified parameters of a servo-valve (Dinca & Corcau, 2013). Based on the numerical data obtained by the authors in (Dinca & Corcau, 2013), one aims to obtain a null steady-state error and a short transient time for our system.

The mathematical model supposes a proportional behaviour of the servo-valve with respect the command current, neglecting its internal dynamic. On the one hand this approximation permits to use the servo-valve model presented in (Dinca & Corcau, 2013), and on the other hand allows a considerable simplification of the numerical simulations.

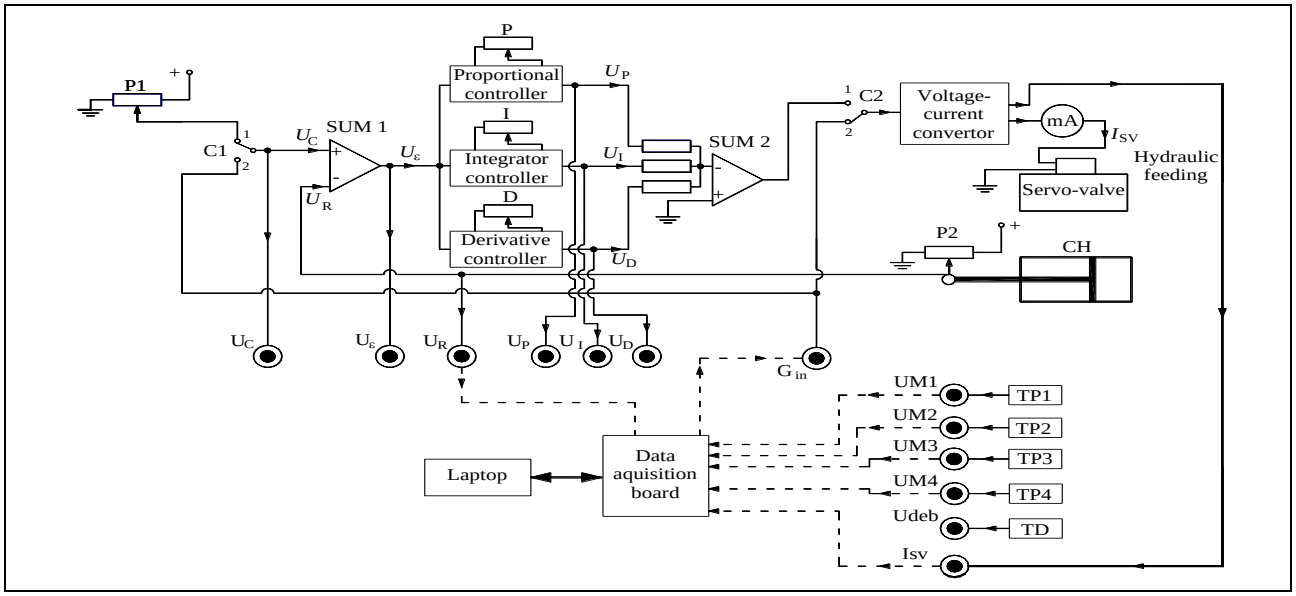

Fig. 1. Experimental system electrical scheme

The developed experimental model is based on the electrical scheme presented in (Dinca & Corcau, 2013), (Dinca et. al., 2010). The servo-actuator command is generated by a laptop. For the control loop closing it is necessary to use the feedback signal U_R which is acquired by a NI-USB 6251 data acquisition card. The signal acquisition is fulfilled using the *Analog input* block from DATA ACQUISITION TOOLBOX. The comparison between the feedback voltage and the generated command is realized in the control scheme developed in MATLAB/SIMULINK and then is computed the command voltage applied to the voltage-current controller using the controllers implemented although in MATLAB/SIMULINK. The output to the data acquisition card is realized using the *Analog Output* block. The voltage from the data acquisition board is applied to the G_{in} terminal, and further, by the C2 switch turned on the position 2 it reach to the voltage-current converter input. In this manner, the scheme works as an electro-hydraulic servo-actuator commanded by a laptop.

2. Mathematical Modeling and Experimental Identification of the Servo-Valve

The hydraulic scheme of the servo-actuator is presented in Fig. 2 (Dinca & Corcau, 2013). One neglected the response time of the torque motor and of the first hydraulic stage of the servo-valve, so they are included in the block T.M. + F.S. which was considered a proportional behaviour.

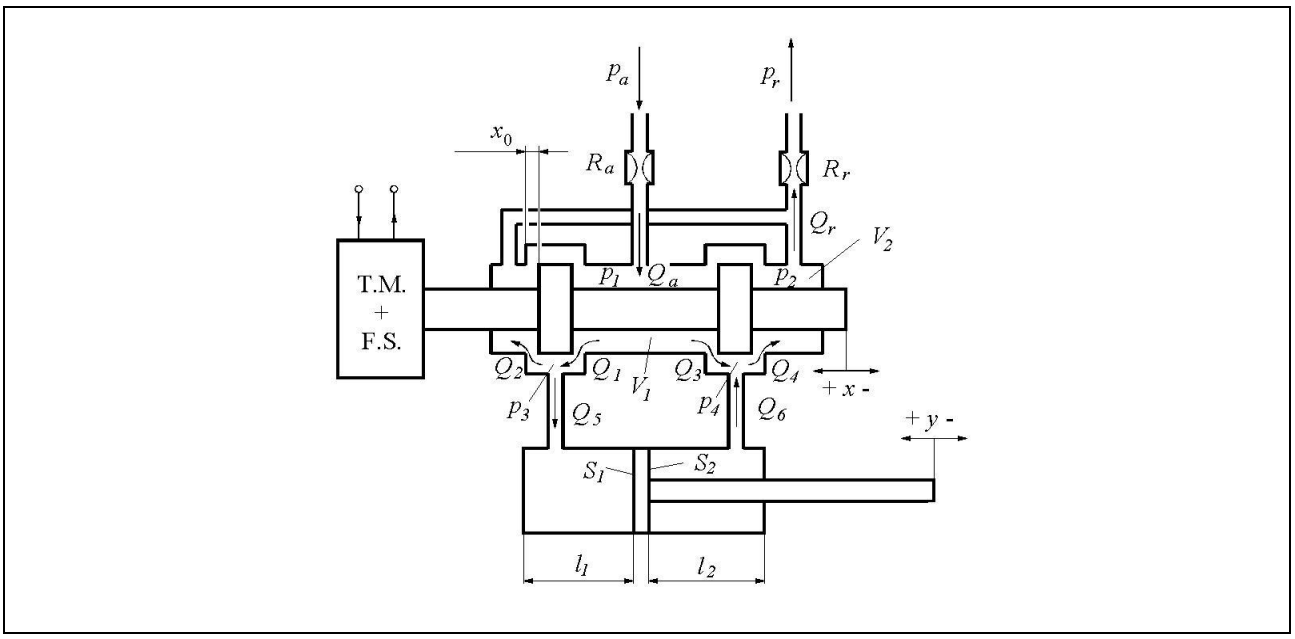

Fig. 2. The model for the hydraulic part of the servo-actuator

For the mathematical model of the servo-actuator one uses the servo-valve model in (Dinca & Corcau, 2013), with the parameters identified by the authors in that work. The piston movement is produced under the action of p_3 and p_4 pressures, which are determined using the state equation of the hydraulic liquid

$$\rho = \rho_0 (1 + \beta \cdot p) \tag{1}$$

where $\beta = 1/E$, E is the coefficient of elasticity of the hydraulic liquid. This equation is applied in fact for the calculus of the pressures p_1 – p_4. In order to determine the pressures p_1 and p_2 one can write the relations for the liquid density in the input and output chambers of the servo-valve. Supposing these volumes equals, $V_1 = V_2 = 3$ cm^3, and, in the initial moment, the liquid masses in these chambers with the expressions

$$m_{10} = \rho_0 (1 + \beta \cdot p_a), \; m_{20} = \rho_0 (1 + \beta \cdot p_r), \tag{2}$$

one can write the time evolution of these masses under the form

$$m_1 = m_{10} + \rho_0 \int_0^t (Q_a - Q_1 - Q_3) \cdot \mathrm{dt} \tag{3}$$

$$m_2 = m_{20} + \rho_0 \int_0^t (Q_2 + Q_4 - Q_r) \cdot \mathrm{dt} \tag{4}$$

From equations (1) to (4) it results

$$p_1 = \frac{1}{\beta}\left(\frac{m_{10} + \rho_0 \int_0^t (Q_a - Q_1 - Q_3)\cdot \mathrm{dt}}{\rho_0 \cdot V_1} - 1\right) \tag{5}$$

$$p_2 = \frac{1}{\beta}\left(\frac{m_{20} + \rho_0 \int_0^t (Q_2 + Q_4 - Q_r)\cdot \mathrm{dt}}{\rho_0 \cdot V_2} - 1\right) \tag{6}$$

In the same manner, one can determine the liquid masses in the hydraulic cylinder chambers, but one may take account the variable volume of these chambers.

$$V_3 = S_3(l_{30} + y),\ V_4 = S_4(l_{40} - y) \tag{7}$$

where l_{30} and l_{40} are the initial lengths of these chambers;

$$m_3 = m_{30} + \rho_0 \int_0^t (Q_1 - Q_2)\cdot \mathrm{dt} \tag{8}$$

$$m_4 = m_{40} + \rho_0 \int_0^t (Q_3 - Q_4)\cdot \mathrm{dt} \tag{9}$$

$$p_3 = \frac{1}{\beta}\left(\frac{m_{30} + \rho_0 \int_0^t (Q_1 - Q_2)\cdot \mathrm{dt}}{\rho_0 \cdot S_3 \cdot (l_{30} + y)} - 1\right) \tag{10}$$

$$p_4 = \frac{1}{\beta}\left(\frac{m_{40} + \rho_0 \int_0^t (Q_3 - Q_4)\cdot \mathrm{dt}}{\rho_0 \cdot S_4 \cdot (l_{40} - y)} - 1\right) \tag{11}$$

with $m_{30} = \rho_0(1 + \beta \cdot p_{30}) \cdot S_3 \cdot l_{30}$ and $m_{40} = \rho_0(1 + \beta \cdot p_{40}) \cdot S_4 \cdot l_{40}$.

It must add to these equations the movement equation for the piston

$$m\frac{\mathrm{d}^2 y}{\mathrm{d}t^2} = p_3 \cdot S_3 - p_4 \cdot S_4 - f \cdot \frac{\mathrm{d}y}{\mathrm{d}t}, \tag{12}$$

where a viscous friction between the piston and cylinder were considered. The servo-actuator studied on the hydraulic bench has no mechanical load, so there is no elastic term.

The flow ratios Q_1 to Q_4 are determined with the relations presented in (Dinca & Corcau, 2013):

$$Q_1 = \mu_d \cdot L \cdot (x_0 + x) \cdot \sqrt{\frac{2}{\rho}} \cdot \sqrt{p_1 - p_3} = \mu_d \cdot L[(x_0 + k \cdot (i - i_{bias}))] \cdot \sqrt{\frac{2}{\rho}} \cdot \sqrt{p_1 - p_3} = \tag{13}$$

$$= (a + b \cdot (i - i_{bias})) \cdot \sqrt{p_1 - p_3},$$

$$Q_2 = \mu_d \cdot L \cdot (x_0 - x) \cdot \sqrt{\frac{2}{\rho}} \cdot \sqrt{p_3 - p_2} = (a - b \cdot (i - i_{bias})) \cdot \sqrt{p_3 - p_2}, \tag{14}$$

$$Q_3 = \mu_d \cdot L \cdot (x_0 - x) \cdot \sqrt{\frac{2}{\rho}} \cdot \sqrt{p_1 - p_4} = (a - b \cdot (i - i_{bias})) \cdot \sqrt{p_1 - p_4}, \tag{15}$$

$$Q_4 = \mu_d \cdot L \cdot (x_0 + x) \cdot \sqrt{\frac{2}{\rho}} \cdot \sqrt{p_4 - p_2} = (a + b \cdot (i - i_{bias})) \cdot \sqrt{p_4 - p_2}. \tag{16}$$

In equations (13) to (16) one have to know if the command current i is in the interval ($-I_{cl}$, I_{cl}) or outside of this. If $i<-I_{cl}$ the slots 2 and 3 are closed, so the flows Q_2 and Q_3 become null. In the same way, if $i>I_{cl}$, then the slots 1 and 4 are closed and the flows Q_1 and Q_4 become null.

For the flows Q_a and Q_r are used the relations

$$Q_a = R_a \sqrt{p_a - p_1}, \tag{17}$$

$$Q_r = R_r \sqrt{p_2 - p_r}. \tag{18}$$

The parameters a , b, I_{cl} , R_a and R_r were experimentally determined in (Dinca & Corcau, 2013). One preferred to use a mathematical model with mass flow ratios which ensure a better stability in the numerical simulations and reflects better the servo-actuator functioning, although is more complicated. One may use a linear model with mass flow ratios which is simple and can be studied easier concerning the system stability, but these models reach sometimes instability zones which are not present in the servo-actuator functioning and so, they do not reflect exactly the servo-actuator behaviour.

One have to add to the relations above the functioning relations of the controller which reflect the dependence between the error voltage U_ε and the controller output voltage U_{reg}, and although the voltage-current converter equation. For the voltage-current converter one may consider very good a proportional dependence between the input voltage and the output current, $i = K_{U-I} \cdot U_{reg}$. From the constructive data one obtained a gain coefficient $K_{U-I} = 10\,\text{mA/V}$. In the laboratory tests one used many types of controllers, but in this chapter are presented only three of them.

The servo-actuator functioning equations were implemented in a MATLAB/SIMULINK scheme, shown in figure 3. In this scheme one used the "Transport Delay" blocks in order to avoid the algebraic loops which may appear in SIMULINK.

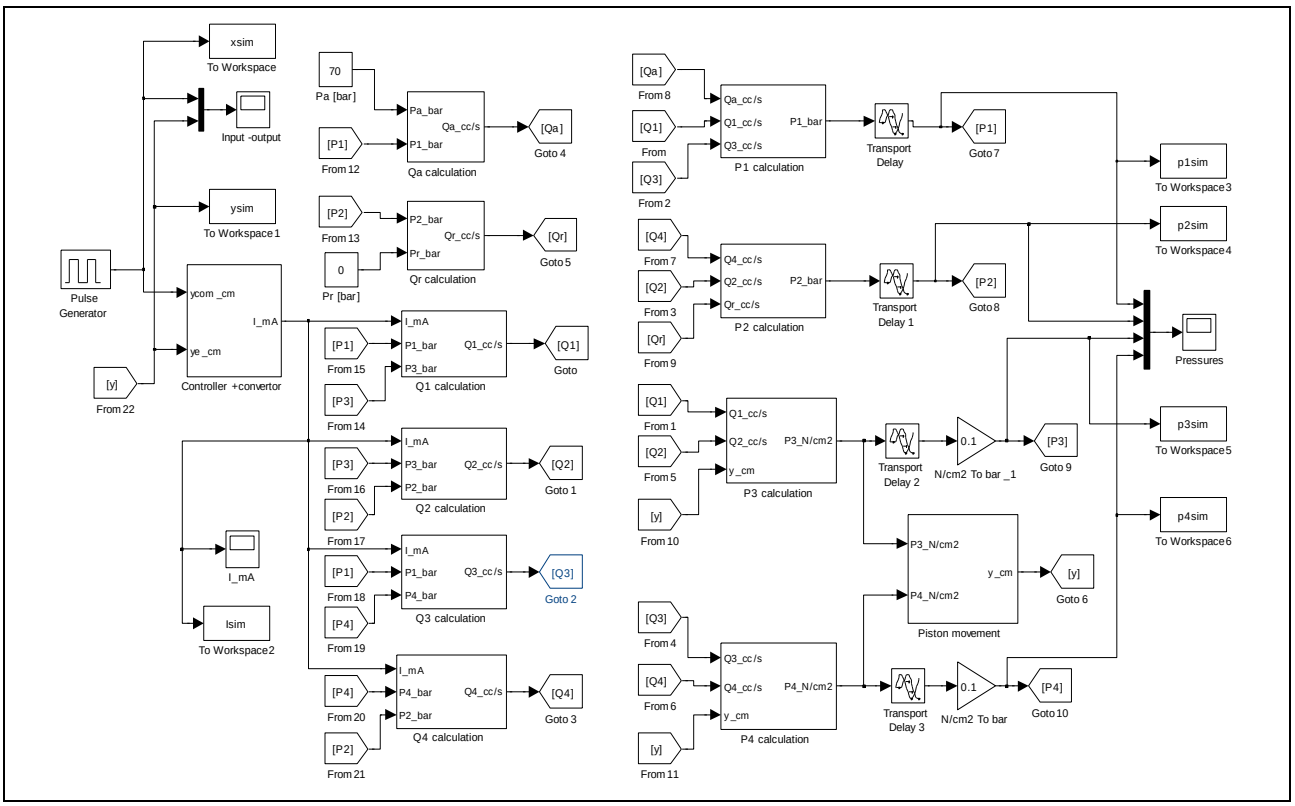

Fig. 3. The simulation scheme for the servo-actuator

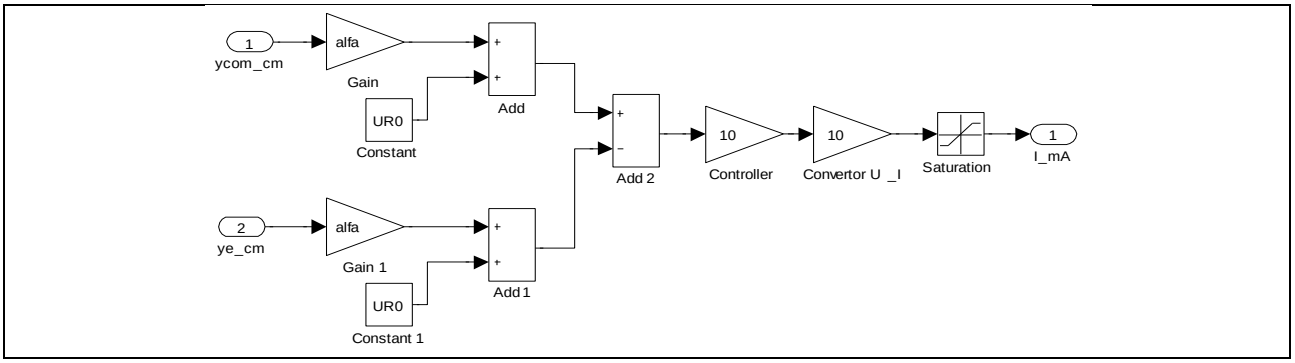

Fig. 4. The structure of the *Controller+converter* block

In figure 4 is presented the *Controller+converter* block whose structure is important for the servo-actuator functioning. It implements the controller and the voltage-current converter. It although performs the conversion of the cylinder rod displacement to the feedback voltage. Although one could implement a controller with displacement inputs - y_{com} and y_e one preferred to convert these displacements in voltages with same values as the experimental ones. In this manner one could use in simulations the same controller blocks as those used in experimental tests without any change. The experimental controller uses obviously the voltages U_C and U_R as inputs. For a 0 cm displacement, the feedback voltage from potentiometer P2 is U_{R0} = 5.75 V, and for a 12.5 cm displacement the feedback voltage is $U_{R12.5}$ = 8.17 V. With these values one could determine the gain α which appear in figure 4 at the displacement-voltage conversion. The conversion equation is

$$U_c[\mathrm{V}] = 5.75 + 0.1936 \cdot y[\mathrm{cm}] \tag{19}$$

3. Experimental Controller Scheme

For the experimental studies one used some controllers implemented in MATLAB/SIMULINK (Fig. 5). The output of the data acquisition card (NI-USB 6251), used to command the voltage-current converter, is sent to the G_{in} terminal, as in figure 2. On the way, the card is used to acquire the feedback voltage U_R obtained from the terminal with the same name as in figure 2. In order to display the displacements of the cylinder rod, one used the inverse relationship of (19). The used sampling frequency was 100 Hz.

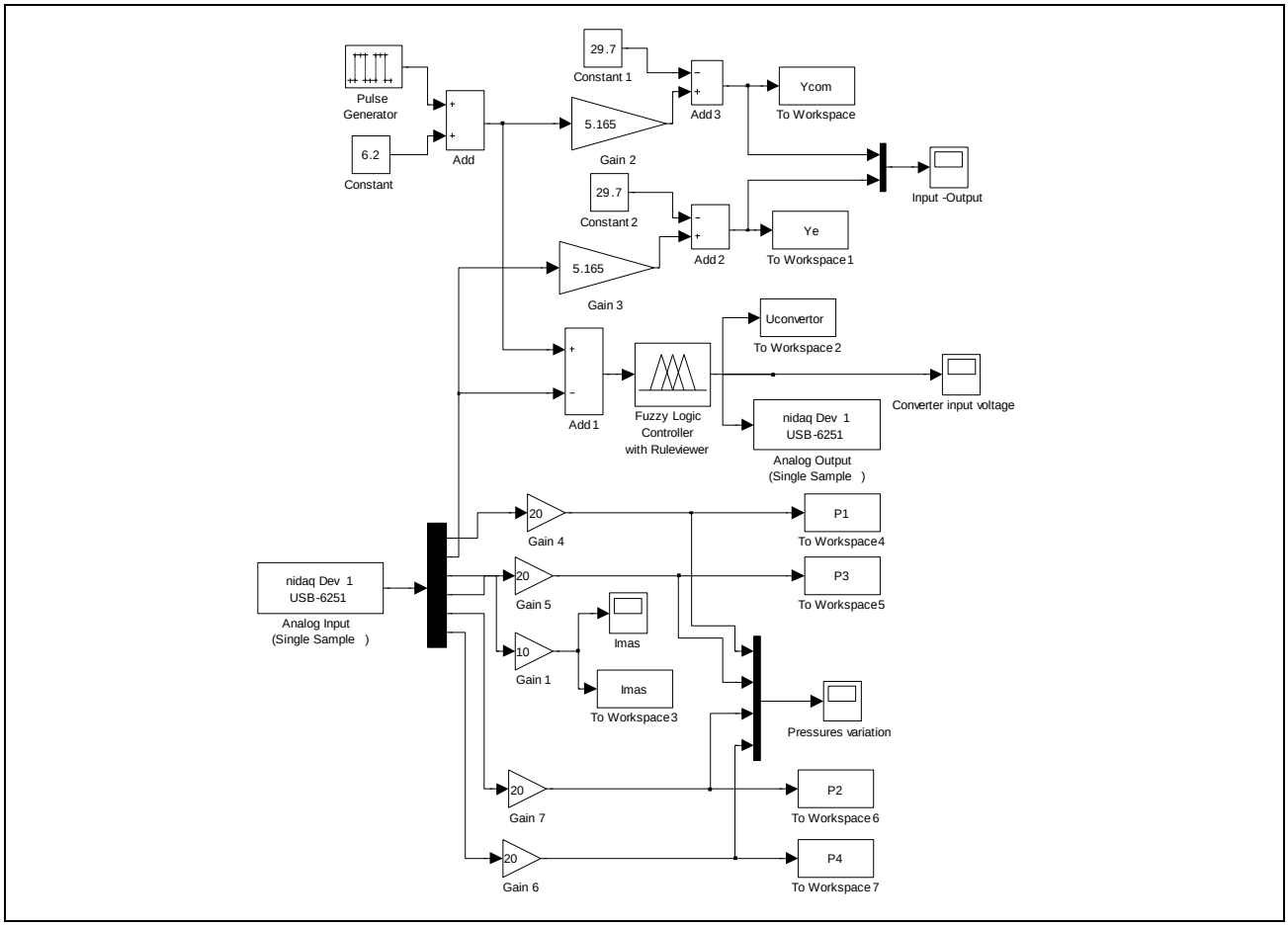

Fig. 5. MATLAB/SIMULINK scheme for experimental study of servo-actuators with different controllers

The command signal is synthesized with a pulse generator block in MATLAB/SIMULINK. This block provides at output pulses with the minimum value 0 and the maximum value prescribed by the user. The maximum value was chosen 1 V, but in order to bring the signal in the command voltage domain accepted by the servo-actuator (between 5.75 and 8.17 V) it was necessary to add an offset voltage. The offset voltage was chosen 6.2 V so the obtained pulse fits better in the command voltage domain. One made although the conversion of the voltage in displacement, like the U_R voltage case, in order to display the input and the output signals of the servo-actuator. These displacements, obtained from U_C and U_R were displayed on a *Scope* virtual instrument and were recorded to *Workspace* for future processing.

Two of the studied controllers were fuzzy logic based, implemented by a *Fuzzy Logic Controller with Ruleviewer* block, and one was proportional type obtained by replacing the fuzzy controller with a gain coefficient.

4. Physical Parameters

For the numerical simulations performed in SIMULINK were used the physical parameters presented in the following. A part of them were measured, others were experimentally determined by the authors in (Dinca & Corcau, 2013), and some of them, concerning the physical properties of the hydraulic liquid were considered based on the medium values in the literature, taking account the used liquid were an additived mineral oil.

Geometrical parameters of the hydraulic cylinder: piston diameter d_p = 3 cm, rod diameter d_t = 1.4 cm, section S_3 =7.068 cm^2 , section S_4 = 5.529 cm^2 , initial left chamber length l_{30} = 2 cm, initial right chamber length l_{40} = 14.5 cm, initial liquid mass in the left chamber m_{30} = 12.040 g, initial liquid mass in the right chamber m_{40} = 68.280 g, piston-rod ensemble mass m = 1 kg, viscous friction coefficient between the piston and cylinder f = 5 Ns/m. Servo-valve parameters: chamber 1 volume V_1 = 3 cm^3, chamber 2 volume V_2 = 3 cm^3, parameter a from relations (13) to (16), experimentally determined $a = 0.2221\,\text{l}/(\text{min}\cdot\sqrt{\text{bar}})$, parameter $b = 0.0600\,\text{l}/(\text{min}\cdot\text{mA}\cdot\sqrt{\text{bar}})$, also experimentally determined, closing current I_{cl} = 3.70 mA, and bias current I_{bias} = 2.83 mA. Hydraulic circuit parameters: liquid density $\rho = 0.85\,\text{g/cm}^3$, elasticity module E=18000 bar, hydraulic resistances $R_a = 47.2298\,\text{cm}^3/\left(\text{s}\cdot\sqrt{\text{bar}}\right)$, $R_r = 69.0677\,\text{cm}^3/\left(\text{s}\cdot\sqrt{\text{bar}}\right)$, feeding pressure p_a = 70 bar, and return pressure p_r = 0 bar. Displacement transducer parameters: null displacement voltage U_{R0} = 5.75 V, 12.5 cm displacement voltage $U_{R12.5}$ =8.17 V, and voltage-displacement slope $\alpha = 0.1936\,\text{V/cm}$. Voltage-current converter slope: $K_{U-I} = 10\,\text{mA/V}$.

5. Proportional Controller with gain *K*=10

The simplest controller is the proportional controller, so it was implemented in MATLAB/SIMULINK by replacing the *Fuzzy Logic Controller with Ruleviewer* block in figure 5 with an amplifier with gain K=10. This value was chosen by successive tests on the test bench. Greater gain values (about 15) lead to servo-actuator auto-oscillations, while smaller values produce response time too big. This value reach a trade between the time response and the stability of the servo-actuator.

The experimental results and the simulated ones are shown in figure 6. In figure 6.a in green is the command signal, in magenta is the measured response, and in blue is the simulated response. In figure 6.b in red is the measured current through the servo-valve coils and in black is the simulated current. In figure 6.c in green is the pressure p_1, in blue the pressure p_2, in magenta is pressure p_3 and in red is the pressure p_4. The darker lines correspond to the simulation and the lighter to the measured data.

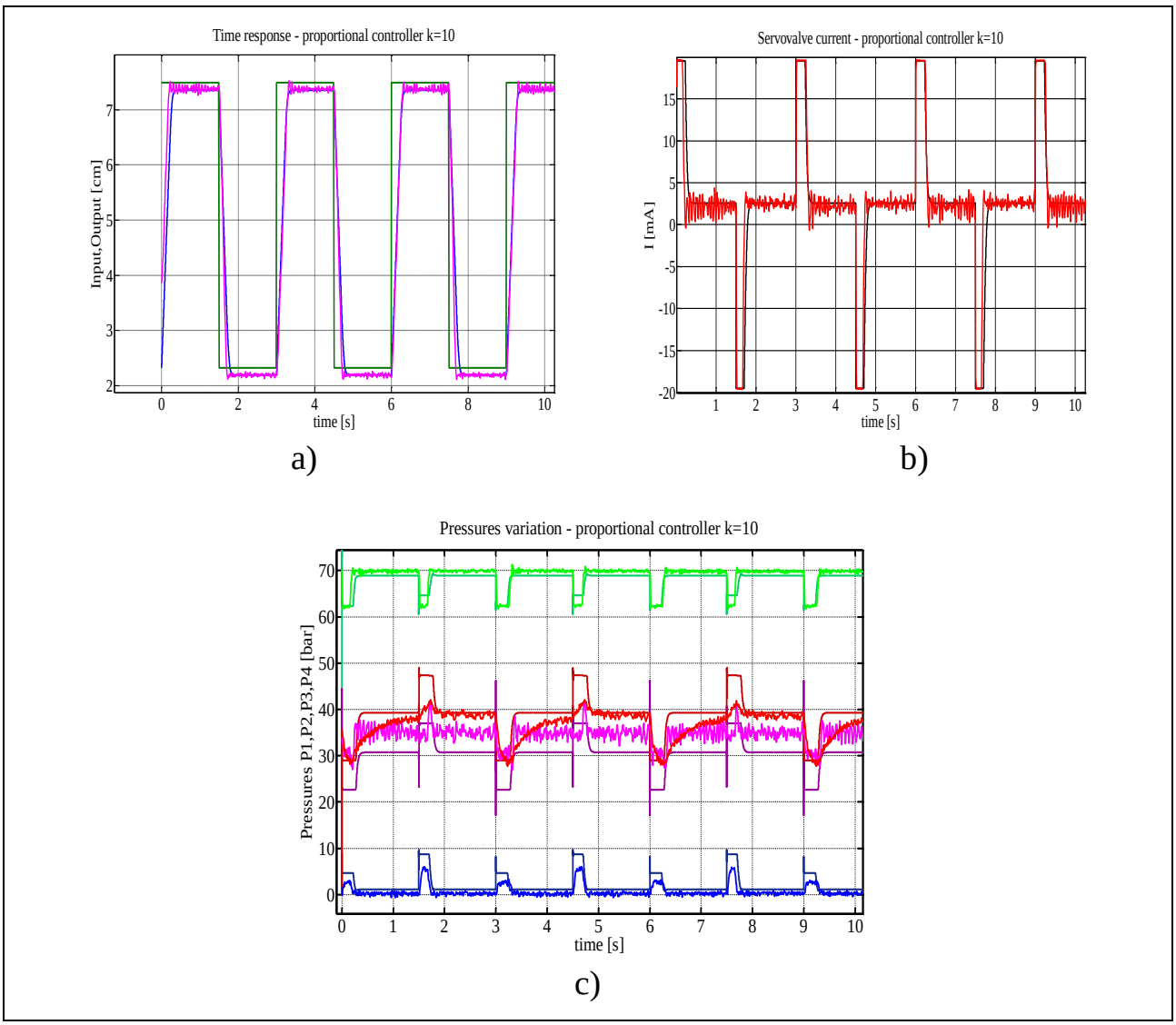

Fig. 6. Functioning of servo-actuator provided with proportional controller

On observe a very good correspondence between the measured and the simulated response and also a very good concordance between the simulated and measured currents. Also, the pressures p_1 and p_2 show a good concordance between the measurements and the simulation, with some greater deviations at the pressure peaks when the servo-valve current is at saturation. The pressures p_3 and p_4 present greater deviations, especially the pressure p_4. One can explain these differences by the presence of some hydraulic resistances in the test bench construction, between the servo-valve and the hydraulic cylinder (relatively long pipes, ramifications for the pressure transmitters and the tap R1 – see (Dinca & Corcau, 2013)) which were neglected in the theoretical model. Also, the dry friction between the piston and cylinder was neglected. This fact could explain the smaller difference between the pressures p_3 and p_4 than it is necessary to ensure the piston equilibrium without dry friction. This could be a way to improve the mathematical model by taking account of mentioned hydraulic resistances and of the dry friction between the piston and the cylinder.

Figure 6.b reveals a pretty long period in which the voltage-current converter is in saturation. In the presented case, the voltage-current converter works practically

only at saturation. One found also a stationary error due to the servo-valve bias especially. One followed to compensate this error using fuzzy logic controllers, which could improve additionally the dynamic behaviour of the system. One improvement could be the reduction of the converter saturation time.

In the development of the following fuzzy controllers, one intent to reach the desired improvements by membership functions adjustment, namely to vanish the stationary error and the saturation period of the converter. One presents in the next sections two fuzzy controllers and the results obtained with these controllers.

6. Fuzzy Controller with Globally Translated Membership Functions on Output

The first targeted improvement in comparison with the proportional controller was to vanish the stationary error by the global translation of the output membership functions. So, the membership functions shape on input and on output was kept the ANFISEDITOR generated one, but one made a global translation of the output membership functions to obtain a null flow when the error voltage is equal with the stationary error in the proportional case. The membership functions and the control surface are shown in figure 7.

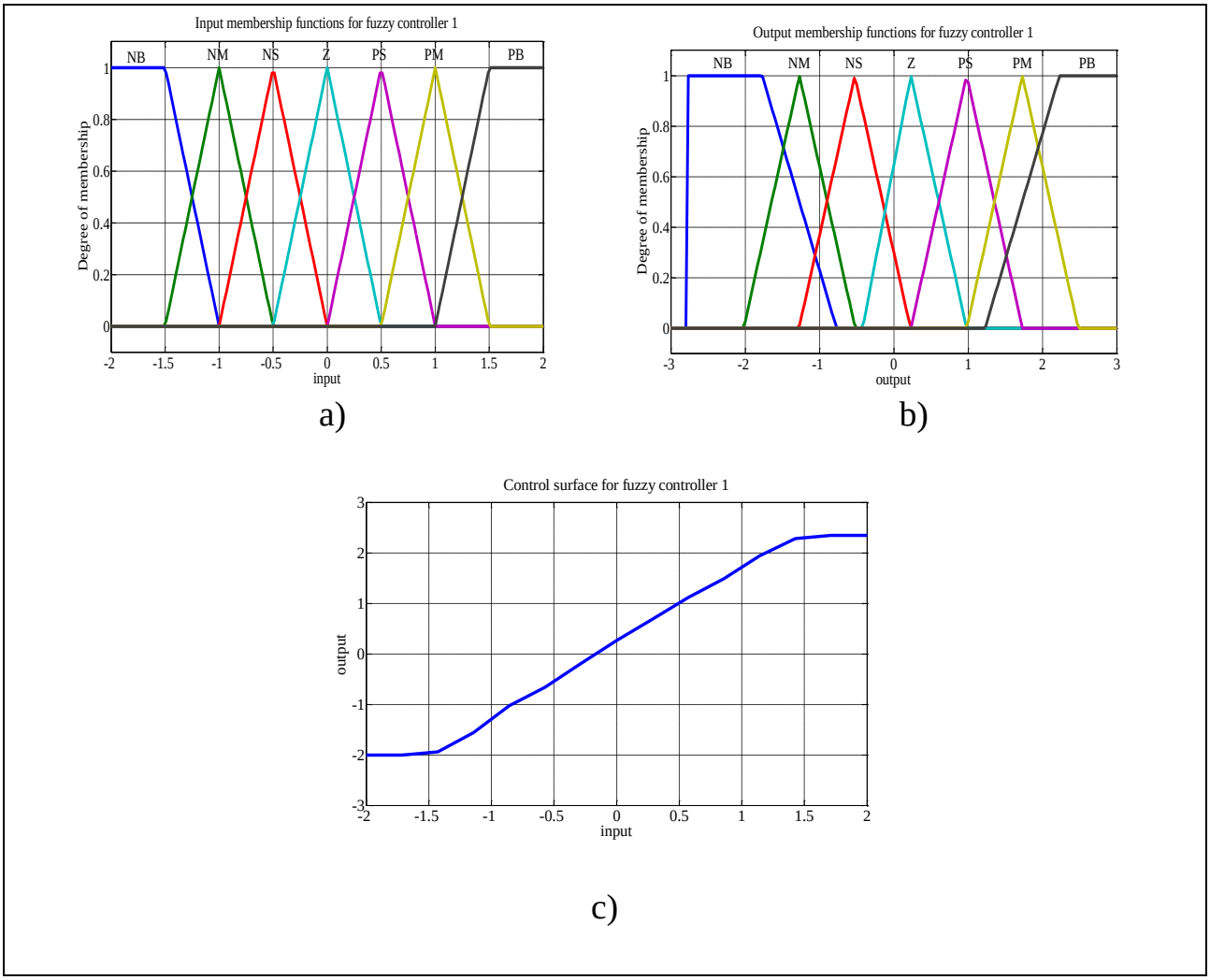

Fig. 7. Membership functions and control surface for the fuzzy controller with globally translated membership functions on output

For the fuzzy controllers development one used Mamdani controllers with 7 membership functions on input and on output. The linguistic terms used were: negative big – NB, negative medium – NM, negative small – NS, zero – Z, positive small – PS, positive medium – PM, and positive big – PB, both on input and output. One chosen triangular shape for the membership functions, excepting the extreme functions – NB and PB which were trapezoidal. The inference laws were the usual: NB input – NB output, NM input – NM output, … , PB input – PB output. The input range was [-2, 2] and the output range was [-3, 3] in order to obtain a greater slope for the control surface and to reduce the response time. One found in the control surface shape it is obtained the desired translation of the null point so the stationary error will be vanished, but the command surface remained linear on the median portion, that means practically a proportional behaviour. With this improvement one obtained only the stationary error vanishing.

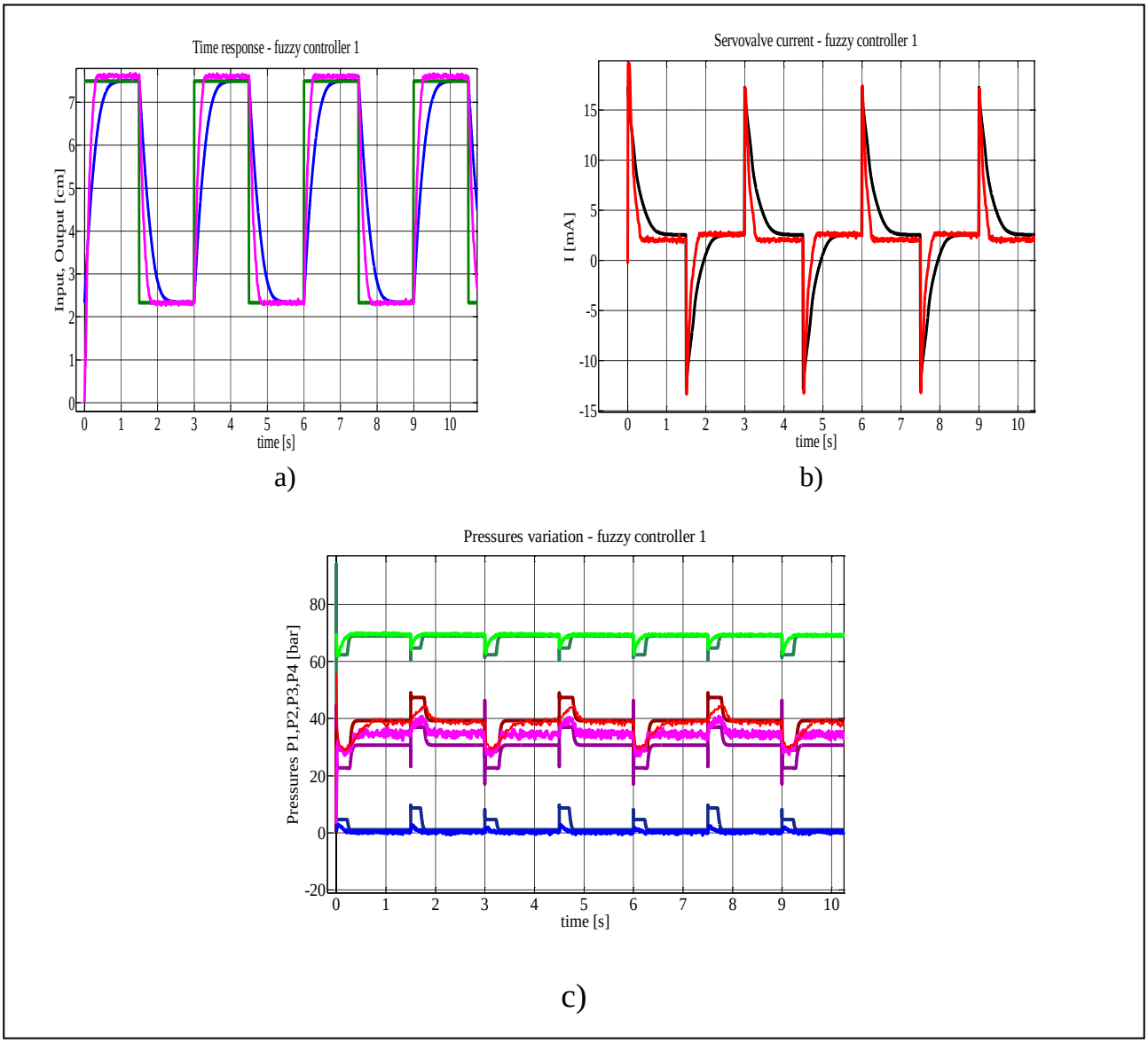

Fig. 8. Functioning of the servo-actuator provided with fuzzy controller with globally translated membership functions on output

For the numerical simulations one used the same fuzzy controller as in the experimental determinations instead of the proportional one in the figure 4. The servo-actuator and mathematical model behaviour is represented in figure 8. One observes an important improvement concerning the servo-valve command current. It does not reach the saturation in any situation. Also the stationary error is vanished on the mathematical model and for the experimental servo-actuator for the lowest value of the displacement. The presence of a very small stationary error at the highest displacement may be explained only by the dry friction presence which has different senses when the piston moves left or right. It was reached a good concordance between the peeks of the command currents in the experimental and simulated data.

Important differences arise in this case between the experimental and the simulated response time. Big enough differences appear also between the experimental and simulated variations of the p_3 and p_4 pressures. Taking into account the command current does not reach saturation one conclude the reason of these difference is due to the hydraulic resistances between the servo-valve and the cylinder which were neglected in the mathematical model. Simulations performed with viscous friction near to zero revealed no improvement of the response time. So, the main source of these important differences remains the mentioned hydraulic resistances.

7. Fuzzy Controller with Modified Membership Functions on Input and Translated Functions on Output

This controller wants to improve the results obtained with the previous controller, namely small response time with null stationary error. In fact, one used modified input functions and a translation of the output membership functions with a value equal with the first fuzzy controller which was realized. The membership functions and the control surface are presented in figure 9.

The servo-actuator behaviour in this case is presented in figure 10. From this figure one can be observed that the new controller improves the behaviour of the previous controller. The stationary error is greatly reduced, remains only dry friction effect and the response time is about 20% reduced in comparison with the first fuzzy controller. The command current reach only for a short period the saturation value and the pressures p_3 and p_4 keep a variation like the second fuzzy controller case. One obtained a good behaviour for the servo-actuator combining two adjustments of the membership functions realized, each one solving one of the servo-actuator problems – stationary error and response time.

One observe a kind of "linear behaviour" of the fuzzy controller which allows to overlap the effects of different adjustments in the membership functions shape – the global displacement of the output membership functions and the modification of the input membership functions. It results a way to construct a fuzzy controller in many steps, at each step solving one problem of the controller and finally overlapping the effects. It would be interesting in the future to study if this method may be used in the design of fuzzy controller which has to fulfil other requirements such limiting the inertia forces or different variations on the actuated element.

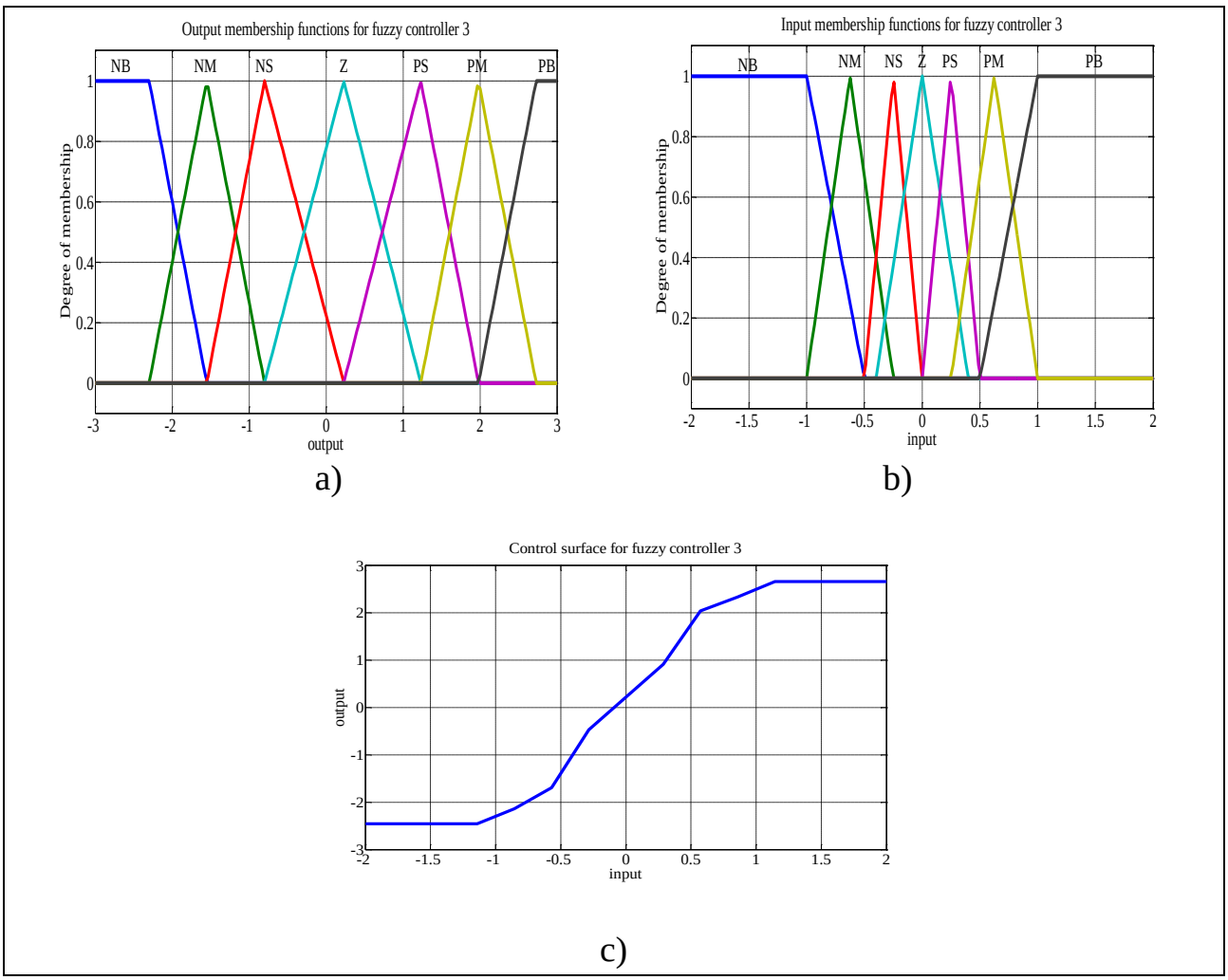

Fig. 9. Membership functions and control surface for the fuzzy controller modified membership functions on input and globally translated on output

Regarding the experimental results and the numerical simulations, it still remains a difference between the two response times. Also, it still remains the differences between experimental and numerical variations of p_3 and p_4 pressures.

One can consider that the mathematical model and the simulation scheme reflect properly the servo-actuator behaviour phenomena and permit to obtain results close to the experimental ones. In figure 10.c one find the pressure p_4 (in red) presents slower experimental variations at the rod withdrawal than the simulated variation and have almost the same slope at the rod extension, even the pressure peaks differ. In the same way, one observes the slower variations of the experimental pressure p_3 at the rod withdrawal and almost the same slope at the rod extension. These slower experimental variations can be obtained only in the presence of some hydraulic resistances between the servo-valve and the cylinder on the test bench, which were neglected in the mathematical model. Another difference between the experiment and the numerical simulation is a smaller difference in the experiment between the pressures p_3 and p_4 in stationary regime. The experimental pressures in the cylinder chambers does not respect the equilibrium relation

$$p_{3r} \cdot S_3 = p_{4r} \cdot S_4 \tag{20}$$

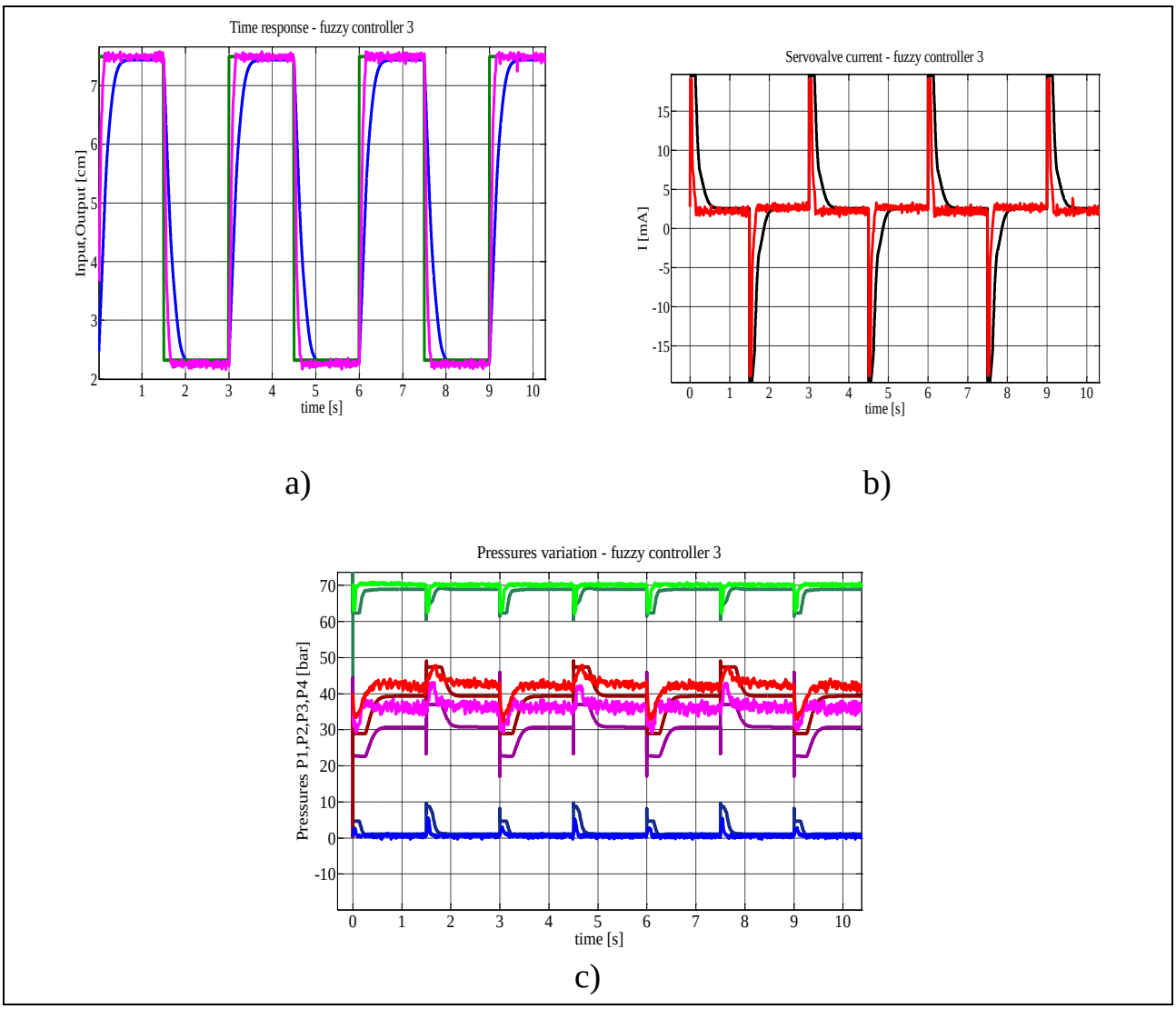

Fig. 10. Functioning of the servo-actuator provided with fuzzy controller with modified membership functions on input and globally translated on output

That means there is another force which is neglected. Because the servo-actuator is tested without load, this force can be only the dry friction between the piston and cylinder. It would be interesting to perform experimental tests with the loaded servo-actuator. Numerical simulations realized in (Dinca & Corcau, 2007) shown for a loaded electro-hydrostatic servo-actuator the dry friction effect is negligible.

8. Conclusion

This paper presents in detail some problems concerning the electro-hydraulic servo-actuators. The studied servo-actuator is experimentally developed on an experimental bench. Some differences appear between the peak pressures in the hydraulic cylinder chambers when the command current of the servo-valve reach values near the saturation due to the hydraulic resistances between the servo-valve and the hydraulic cylinder present in the test bench construction. Another important difference between the numerical simulations and experimental data is due to the dry friction between the piston and cylinder. In the numerical simulations the dry friction

were neglected. In experimental tests, this friction induced in the cylinder chambers, pressures which do not respect the equilibrium equation without dry friction. But this effect can become negligible in load conditions. As it is observed in the simulations performed in other works (Dinca & Corcau, 2007), the presence of a load force, about tens of daN, may drop substantially the effect of the dry friction and to obtain a good concordance between the experience and the numerical simulations. The mathematical model of the servo-actuator was obtained using mass flow ratios in order to obtain a better numerical stability. The mass flow ratio model is recommended to verify the behaviour of a servo-actuator, while the linear model with volume flow ratios is useful to design a servo-actuator. The linear model leads to covering conditions concerning the servo-actuator stability. In this case we followed to obtain a better concordance between the numerical simulations and the experimental data, so we used the mass flow ratio model. For the control loop closing one tested different controllers implemented in MATLAB/SIMULINK. The tests were performed both experimentally and numerically. A proportional controller and two fuzzy controllers were tested. In the proportional case, a gain $K=10$ was used. One obtained a good concordance between experiments and simulation for the response times and the command current, but some differences appeared for the pressures variations due to the reasons mentioned before. An inconvenience for this controller is the long period the command current reach the saturation, so it needs a higher control power. This power is negligible on an aircraft but may be important on a spatial vehicle.

Another problem for the proportional controller is it does not compensate the servo-valve bias current, so one obtains a relatively large stationary error. In order to compensate the stationary error and to reduce the response time while reducing the control power, two fuzzy controllers were tested. The fuzzy controllers permit easy to obtain effects like stationary error compensation, time response decrease, inertia forces diminishing in the acceleration-brake process, etc. The prize for this advantage is the necessity of a higher computing power than a proportional or proportional-integrator controller implementation and the impossibility to implement fuzzy controllers with analog devices which are simpler.

The first studied fuzzy controller followed to eliminate the stationary error by the global displacement of the output membership functions. The results were very good both numerical and experimental, but an important difference appeared in the response times. One put these differences on the reasons mentioned before. The second fuzzy controller eliminated the stationary error and reduced the response time. One obtained this effect using the modified input membership functions and the output functions of the first controller. The results fulfilled the expectations, reaching a good behaviour of the servo-actuator. For the future works, it would be interesting to obtain experimental data for the on load behaviour of the servo-actuator. By this way one may appreciate the importance of the neglected terms (dry friction and some hydraulic resistances) in these situations. A second study direction would be the identification of the neglected parameters and to improve the mathematical model.

9. References

Ciupitu, L.; Brotac, S. & Ivanescu, N. A. (2011). On the Controlling of the Coilers from a Metal Extrusion Press, *Annals of DAAAM for 2011 & Proceedings of the 22nd International DAAAM Symposium*, 23-26th November 2011, Vienna, Austria, Volume 22, No. 1, ISSN 1726-9679, ISBN 978-3-901509-83-4, Katalinic, B. (Ed.), pp. 0345-0346, Published by DAAAM International Vienna, Vienna

Daachi, B. et al. (2001). A Stable Neural Adaptive Force Controller for Hydraulic Actuator, Proc. IEEE Int. Conf. On Robotics and Automation, Seoul, Korea

Dinca, L., & Corcau, J. (2007). Hydrostatic servo-actuator for aircraft – Research report for the first stage. Research grant 81-036/2007 funded by Romanian Education and Research Ministry, leader INCAS Bucharest

Dinca, L., & Corcau, J.I. Experimental identification of some servovalve parameters used in an electro-hydraulic servoactuator development. Chapter in DAAAM International Scientific Book 2013, Published by DAAAM International, ISBN 978-3-901509-94-0, ISSN 1726-9687, Vienna, Austria

Dinca, L., Lascu, M., Ivan, M., Budau, I., & Sarbu, D. (2010). Hydrulic bench for electro-hydraulic servoactuators and servo-valves testing. *Annals of University of Craiova, Electrical Engineering Series*

Dinca, L. (2005). Numerical simulation of hydraulic and pneumatic systems for aircraft – PhD. Thesis, University "Politehnica" Bucharest

Hanzálek, Z., Hospodář, P., Hromčík, M., Waszniowski, L., & Doubrava J. (2009). Hardware in the Loop Simulation of FBW components. AIAA Modeling and Simulation Technologies Conference, Chicago, Illinois

Hietala, J.P., Aaltonen, J., Koskinen, K. T. & Vilenius, M. (2009) Modelling and Simulation of the Aircraft Rudder Hydraulic Servo Actuator with Dynamic Interconnections to Flight Dynamics and Flight Control System Models**.** The 11 th Scandinavian International Conference on Fluid Power, Sweden

Johnsen, S., & Thielecke F. (2011). Integration analysis of trimmable horizontal stabilizer actuators and technology evaluation. *CEAS Aeronaut J*, 2:11–19

Jong-Hwei Wei & Yung-JianWang. (2010). The Digital Adaptive Control System Design of a Hydraulic Servoactuator. *Journal of Aeronautics, Astronautics and Aviation*, Series A, Vol.42, No.3

Mare, J. C. (2009). Comparative Analysis of Energy Losses in Servo-Hydraulic, Electro-Hydrostatic and Electro-Mechanical Actuators**.** The 11 th Scandinavian International Conference on Fluid Power, Sweden

Mizioka, L.S., & Marco Antonio de Oliveira Jr. (2009). Hydraulic fluid validation through modeling and simulation of a servo actuator system**.** Brazilian Symposium on Aerospace Eng. & Applications

Mikhaylov, M.; Larchikov, I. A.; Yurov, A. V.; Cvetkov, V. & Stazhkov, S. (2011). Hydromechanical Constant Speed Drive Forwind-Driven Generators, Annals of DAAAM for 2011 & Proceedings of the 22nd International DAAAM Symposium, 23-26th November 2011, Vienna, Austria, Volume 22, No. 1, ISSN 1726-9679, ISBN 978-3-901509-83-4, Katalinic, B. (Ed.), pp. 0235-0236, Published by DAAAM International Vienna, Vienna

Nakata, N. & Xi Zhao (2011). Numerical Simulation of Model-Based Control Strategy for Hydraulic Actuators**.** (2011). The 6th International Workshop on Advanced Smart Materials and Smart Structures Technology ANCRiSST 2011, Dalian, China

Niksefat, N., & Sepehri, N. (2000). Design and experimental evaluation of a robust force controller for an electro-hydraulic actuator via quantitative feedback theory. *Control Engineering Practice* 8 pp. 1335-1345, www.elsevier.com

Panagiotis, C. (2002). Design, Modeling and Control of a High-Performance Electrohydraulic Servosystem, Master Thesis, in Greek, NTUA

Panagiotis, C., & Papadopoulos, E. (2003). On model-based control of hydraulic actuators. Proceedings of RAAD'03, 12th International Workshop on Robotics in Alpe-Adria-Danube Region Cassino

Precup, R.E., & Preitl, S. (2005). On the Stability and Sensitivity Analysis of Fuzzy Control Systems for Servo-Systems. Springer-Verlag Berlin Heidelberg;

Prodan, D.; Bucuresteanu, A. M. & Balan, E. (2011). Heavy Machine-Tools: Modularized Hydraulic Installations, Annals of DAAAM for 2011 & Proceedings of the 22nd International DAAAM Symposium, 23-26th November 2011, Vienna, Austria, Volume 22, No. 1, ISSN 1726-9679, ISBN 978-3-901509-83-4, Katalinic, B. (Ed.), pp. 0209-0210, Published by DAAAM International Vienna, Vienna

Richard, P. (2005). *DSP Control of Electro-Hydraulic Servo Actuators***.** *Application Report SPRAA76*, Texas Instruments

Rydberg, K. E. (2008). Hydraulic servo systems**.** Linköpings universitet. TMHP51 IEI / Fluid and Mechanical Engineering Systems

Ursu, I., & Ursu, F. (2005). Airplane ABS control synthesis using fuzzy logic**,** *Journal of Intelligent & Fuzzy Systems*, 16, 1, pp. 23–32

Ursu, I., Tecuceanu, G., Toader, A., & Calinoiu, C. (2011). Switching neuro-fuzzy control with antisaturating logic. experimental results for hydrostatic servoactuators. Proceedings of the Romanian Academy**,** Series A, Volume 12, Number 3, pp. 231–238

Ursu, I., Tecuceanu, G., Ursu, F., & Toader, A. (2007). Nonlinear control synthesis for hydrostatic type flight controls electrohydraulic actuators. Proceedings of the International Conference in Aerospace Actuation Systems and Components, Toulouse, June 13–15, pp. 189–194

Ursu, I., Ursu, F., Halanay, A. & Safta, C. A.(2008). Equilibrium stability of a servo actuating flight controls in a servoelastic framework. *Acta Universitatis Apulensis*, no 15

Vasiliu, N., Calinoiu, C., & Vasiliu D. (2009) Improving the accuracy of the electrohydraulic servomechanisms by additional feedbacks. Proceedings of the Romanian Academy, Series A, Mathematics, Physics, Technical Sciences, Information Science, 10, *3*, pp. 277–284

Yu Hong, Feng Zheng-Jin, & Wang Xu-Young, (2003). Nonlinear control for a class of hydraulic servo system. Journal of Zhejiang University SCIENCE, ISSN 1008-3095

*** (2013) http://www.moog.com/search/?q=servovalve++user+manual&site